

Minimum weight design of vertically vibrating 3-D machine foundation coupled to layered half-space¹

Zbigniew Sienkiewicz

Department of Civil and Environmental Engineering

Technical University of Koszalin

Racławicka 15/17, 75-620 Koszalin, Poland

Bogdan Wilczyński

Department of Mechanical Engineering,

Technical University of Koszalin

Racławicka 15/17, 75-620 Koszalin, Poland

(Received September 5, 1997)

Dynamic optimization problem for a machine rigid block foundation on an inhomogeneous soil is considered. The soil deposit under the base of block corresponds to a layer with linearly varying properties overlying a uniform half-space. Furthermore, the block may be surrounded by a backfill. The optimal designs of a vertically excited rectangular block foundation are found by iterative application of a sequential linear programming for a number of rationally inhomogeneous supporting media as well as for a uniform half-space. It illustrates the problem of adequate modelling of the nature of the soil profile and provides an insight into the action of the soil-foundation-machine system from the point of view of the long-term satisfactory performance and safety.

1. INTRODUCTION

Generally, the design of machine foundations is a trial-and-error procedure that should lead to a safe and economical foundation block satisfying the operational requirements of machinery and installations and structural and psychological criteria [16]. A successful machine foundation design requires a systematic using of principles of soil engineering, soil dynamics and theory of vibration [9, 17]. The engineering decision-making process may be helped by structural optimization techniques [1, 3, 15, 27]. Optimization of footings under static loads has been presented by Filipow *et al.* [6], Garstecki [8], Huang and Hiduja [11], Truman and Hoback [28] and Chi and Dembicki [5]. Dynamic optimization of a rigid block resting on a stochastic Winkler medium was considered by Szymczak [26]. More complex problems accounting for the dynamic interaction between the rigid block foundation and the supporting soil deposit have been solved by Sienkiewicz and Wilczyński [20-23]. If machine foundations are constructed as rigid concrete blocks, their response to dynamic loads is completely determined by dynamic properties of the underlying soil deposit. Then, the necessity of careful modelling of unbounded supporting medium properly distinguishes soil dynamics from structural dynamics. For many years, properties of subsoil were evaluated on the basis of the subgrade modulus being soil stiffness per unit area. This concept has been abandoned in advanced engineering practice and nowadays, the dynamic properties are usually described in terms of complex-valued, frequency dependent impedance functions [9]. In the papers [20-23], the dynamic properties of soil medium were described in terms of complex-valued and frequency

¹ Partially presented at The XIII Polish Conference on Computer Methods in Mechanics, Poznań, Poland, 5-8 May, 1997

dependent impedance functions of a homogeneous half-space. The most significant disadvantage of the homogeneous elastic half-space model of soil is that it yields a very large radiation damping for the vertical mode of vibration. In this case, overcritical damping is predicted for most larger machine foundations and the response analysis may considerably underestimate the real vertical vibration amplitude. It is a crucial problem from the point of view of performance and safety of the machine-foundation structural system. Note that in real soils the confining pressure increase with depth due to the overburden even for deep structurally homogeneous deposits of uniform sand or clay. Then, the shear wave velocity and the dynamic shear modulus increase with depth depending upon the type of soil [7, 17]. The problem of minimum weight design of a vertically vibrating machine foundation on an inhomogeneous soil has been solved by Sienkiewicz and Wilczyński [24] for a soil model corresponding to a layer with constant elastic properties overlaying a uniform elastic half-space. In this study, the problem is considered for a more general model of soil corresponding to a layer with linearly varying shear wave velocity overlying a uniform half-space, [25]. The results in each case are compared with those obtained for uniform supporting medium. It provides an insight into the action of the machine-block-soil system from the point of view of safety and long-term adequate performance.

2. ANALYSIS MODEL

A dynamic system consists of a machine on a rigid rectangular block perfectly bonded to a layered half-space. The block may be partially embedded in the ground (Fig. 1). Dynamic soil-foundation interaction is performed by the substructure method in which the system is divided into two substructures. The governing equations are developed separately and then are combined due to conditions of equilibrium and compatibility at the foundation-soil interface, [10].

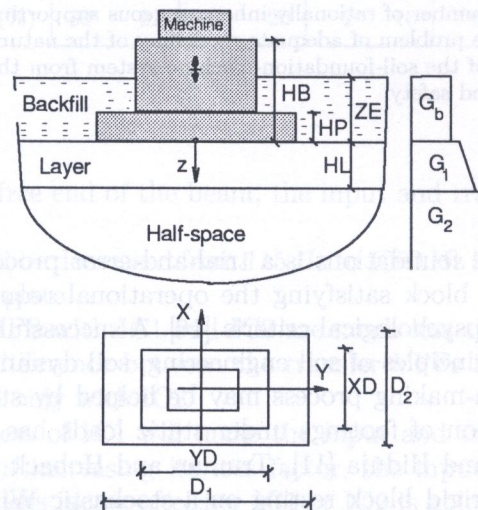


Fig. 1. Machine-foundation resting on a layered elastic soil

2.1. Substructure 1: machine-foundation system

The equation of vertical motion of rigid machine-block system for small amplitude is

$$m\ddot{u}_z(t) = P_z(t) + R_z(t), \quad (1)$$

in which m is the total mass of the block and machine, $u_z(t) = u_z \exp(i\omega t)$ is the uniform harmonic settlement, $P_z(t) = P_z \exp(i\omega t)$ is the harmonic external force, $R_z(t) = R_z \exp(i\omega t)$ is the dynamic soil reaction, ω is the circular frequency and $i = \sqrt{-1}$.

2.2. Substructure 2: supporting medium

The semi-infinite elastic medium is excited by a harmonic vertical force $R_m(t) = R_m \exp(i\omega t)$ acting through the centroid of the base of a massless embedded rigid block. The displacement field in the medium, $u_x(x) \exp(i\omega t)$, $u_y \exp(i\omega t)$, $u_z(x) \exp(i\omega t)$ must satisfy the Navier equations of motion in each layer, the continuity conditions across layer interfaces, the condition of vanishing tractions on the free surface of the half-space, the radiation conditions at infinity and the following condition at the soil-foundation interface Γ :

$$\begin{aligned} u_x(x) \exp(i\omega t) &= 0, \\ u_y(x) \exp(i\omega t) &= 0, \\ u_z(x) \exp(i\omega t) &= u_m \exp(i\omega t), \quad x \in \Gamma = \Gamma_b \cup \Gamma_s, \end{aligned} \quad (2)$$

where $u_m \exp(i\omega t)$ is the uniform vertical dynamic settlement of a rigid massless block, and Γ_b , Γ_s are the horizontal and vertical interface, respectively.

The solution of the radiation boundary-value problem gives the distribution of the traction $T_z^n(x) \exp(i\omega t)$ at the interface Γ that leads to the reaction force $R_m \exp(i\omega t)$

$$R_m \exp(i\omega t) = \int_{\Gamma_b \cup \Gamma_s} T_z^n(x) \exp(i\omega t) d\Gamma(x) = R_b \exp(i\omega t) + R_s \exp(i\omega t), \quad (3)$$

where $R_b \exp(i\omega t)$ is the base reaction and $R_s \exp(i\omega t)$ is the side reaction. Due to the difficulty of obtaining rigorous solution, the contact reaction load on the half-space has been determined by an approximate approach in which it is assumed that the tractions on the horizontal interface Γ_b are equal to those of a rigid massless plate bonded to the surface of a half-space, while the tractions at the vertical interface Γ_s result from the action of an independent sidelayer under the cylindrical plane strain condition [19].

The distribution of base traction can be determined using the integral representation of the surface vertical displacement field

$$u_z(x) \exp(i\omega t) = \int_{\Gamma_b} G_{zz}(x - \xi) \exp(i\omega t) T_z^n(\xi) d\Gamma(\xi), \quad (4)$$

where $G_{zz}(x - \xi) \exp(i\omega t)$ corresponds to the Green's function, which gives the surface vertical displacement of the half-space at a point x due to a harmonic vertical unit force $1 \exp(i\omega t)$ acting at a point ξ . Including the condition of a rigid body motion (2) leads to the integral equation of the Fredholm type of the first kind having Green's function as kernel. The unknown of the integral equation is the distribution of amplitudes of vertical traction T_z^n in the contact area Γ_b . To solve the equation, the contact area Γ_b is subdivided into a number of subregions Γ_n , $n = 1, \dots, N$ and it is assumed that the contact stresses are uniformly distributed within the small subregions Γ_n . Imposing the displacement boundary condition of a rigid plate motion at the centers of the N subregions leads to a linear algebraic equation system for the unknown complex-valued amplitudes of traction at the interface $\Gamma_b = \cup_{n=1}^N \Gamma_n$. Finally

$$\int_{\Gamma_b} T_z^n(x, i\omega) \exp(i\omega t) d\Gamma(x) = \tilde{K}_v^o(i\omega) u_m \exp(i\omega t), \quad (5)$$

where $\tilde{K}_v^o(i\omega)$ is the complex-valued vertical dynamic impedance function of the half-space with constraints imposed by a surface massless rigid plate.

The distribution of traction at the vertical interface Γ_s has been determined by analytical solution of an elastodynamic boundary-value problem of an infinite elastic space subjected to harmonic vertical vibration from a rigid, infinitely long circular inclusion [14]. It can be shown that

$$\int_{\Gamma_s} T_z^n(x, i\omega) \exp(i\omega t) d\Gamma(x) = \tilde{K}_v^s(i\omega) u_m \exp(i\omega t), \quad (6)$$

where $\tilde{K}_v^s(i\omega)$ denotes the complex-valued vertical dynamic impedance function of the backfill.

Combining Eqs. (3–5) and (6) gives

$$R_m(i\omega) \exp(i\omega t) = \tilde{K}_v(i\omega) u_m \exp(i\omega t), \tag{7}$$

where

$$\tilde{K}_v(i\omega) = \tilde{K}_v^o(i\omega) + \tilde{K}_v^s(i\omega). \tag{8}$$

The complex-valued vertical impedance function of the supporting medium can be written in the form

$$\tilde{K}_v(i\omega) = K'_v(\omega) + iK''_v(\omega) = K_v(\omega) + i\omega C_v(\omega), \tag{9}$$

where the real part of the complex-valued impedance function $K'_v(\omega)$ represents the contribution of the force component that is in phase with the motion, whereas the imaginary part $K''_v(\omega)$ represents the contribution of the component that is 90° out of phase. In an equivalent spring-dashpot representation of the supporting medium the stiffness of the spring is given by $K_v(\omega) = \text{Re}(\tilde{K}_v(i\omega)) = K'_v(\omega)$ and the dashpot coefficient is given by $C_v(\omega) = \text{Im}(\tilde{K}_v(i\omega))/\omega = K''_v(\omega)/\omega$. The damping accounts for energy dissipation in subsoil stemming from wave propagation (radiation damping). In contrary to structural dynamics, the equivalent stiffness and damping coefficients depend on the frequency and they are also affected by soil material damping.

To illustrate the characteristics of the vertical impedance function for rigid massless block embedded to a depth ZE in a soil, the case of a rectangular foundation $2B \times 2L$, $B \leq L$, is considered (Fig. 2).

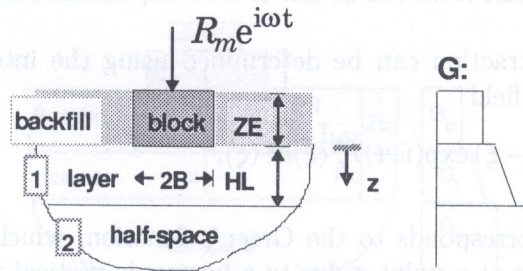


Fig. 2. Rigid massless block embedded in a soil

The soil under the base of block consists of a layer of constant thickness HL bonded to an underlying uniform half-space. The elastic layer is characterized by the density ρ_1 , Poisson’s ratio ν_1 , hysteretic damping constants ζ_{1s} and ζ_{1p} for distortional and dilatational waves, respectively and a distribution of shear modulus with depth $G_1(z)$

$$G_1(z) = G_1(0) \left[1 + (CR - 1) \frac{z}{HL} \right]^2, \tag{10}$$

where $CR = \sqrt{G_1(HL)/G_1(0)}$. It corresponds to linearly varying shear wave velocity of the layer.

The underlying homogeneous elastic half-space is characterized by the density ρ_2 , Poisson’s ratio ν_2 , constant shear modulus G_2 and hysteretic damping constants ζ_{2s} and ζ_{2p} . The backfill is characterized by its density ρ_b , Poisson’s ratio ν_b , constant shear modulus G_b and hysteretic damping constants ζ_{bs} and ζ_{bp} .

For the considered supporting medium, the complex-valued vertical impedance function can be written in the form

$$\tilde{K}_v(i\omega) = G_1(0)B [k_{vv} + ia_0c_{vv}], \tag{11}$$

where k_{vv} is the normalized stiffness coefficient, c_{vv} is the normalized damping one and $a_0 = \omega B \sqrt{\rho_1/G_1(0)}$ denotes the dimensionless frequency. The normalized stiffness and damping coefficients depend on a_0 , L/B , ZE/B , HL/B , $G_b/G_1(0)$, $G_1(HL)/G_1(0)$, $G_2/G_1(HL)$, ρ_b/ρ_1 , ρ_2/ρ_1 , ν_b , ν_1 , ν_2 , ζ_{bs} , ζ_{bp} , ζ_{1s} , ζ_{1p} , ζ_{2s} and ζ_{2p} .

The non-dimensional stiffness and damping coefficients have been calculated for $a_0 \in [0.1, 3]$; $L/B \in [1, 2]$; $ZE/B = 0, 1$; $HL/B \in [2, 10] \cup \infty$; $G_b/G_1(0) = 1$, $G_1(HL)/G_1(0) \in [1, 10.5625]$; $G_2/G_1(HL) = 1.13$; $\rho_b/\rho_1 = 1$; $\rho_2/\rho_1 = 1.13$; $\nu_b = \nu_1 = \nu_2 = 0.33$; $\zeta_{bs} = \zeta_{bp} = \zeta_{1s} = \zeta_{1p} = 0.05$; and $\zeta_{2s} = \zeta_{2p} = 0.03$ and the part of the results is presented in the Figs. from 3 to 10. The results show the effect of the frequency of motion and of the geometry of the contact area and soil profile on the dynamic properties of the supporting subsoil. The Green's function for a layered half-space was determined by the procedure described by Luco and Apsel [13] and the results were obtained by subdividing the base contact area into 64 rectangular subregions and using Gaussian quadrature to evaluate influence functions.

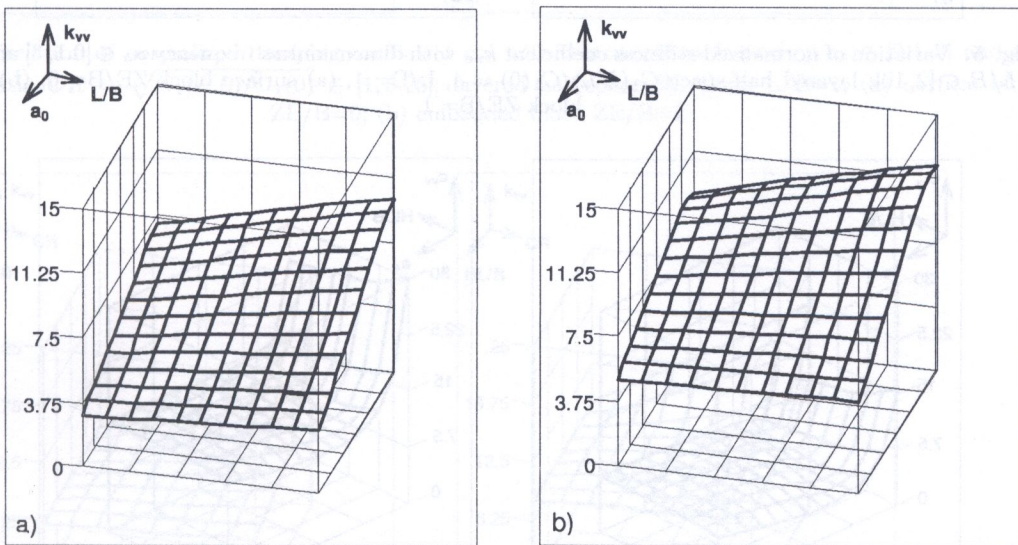


Fig. 3. Variation of normalized stiffness coefficient k_{vv} with dimensionless frequency $a_0 \in [0.1, 3]$ and aspect ratio $L/B \in [1, 2]$; uniform half-space $HL/B = \infty$, (a) surface block $ZE/B=0$; (b) embedded block $ZE/B=1$

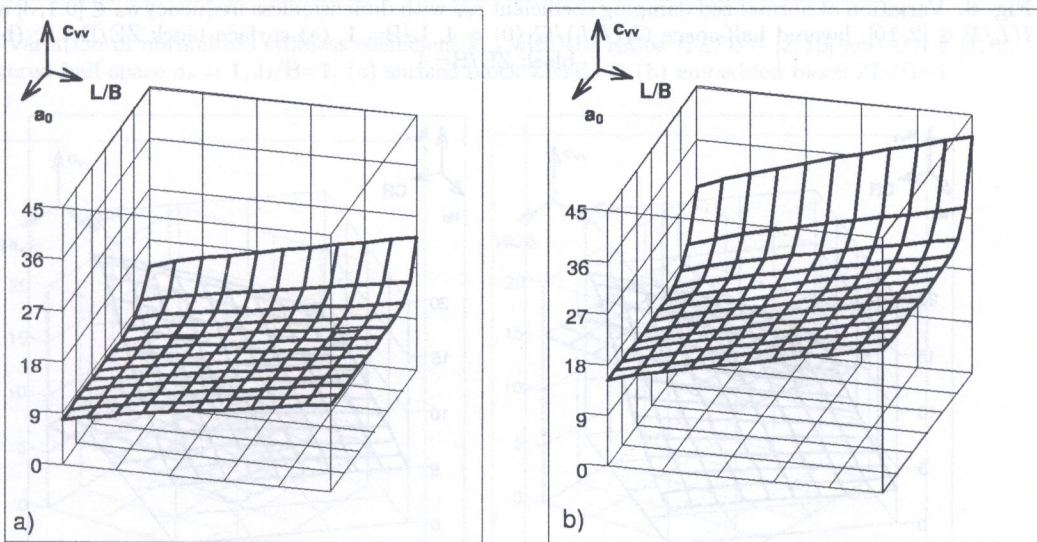


Fig. 4. Variation of normalized damping coefficient c_{vv} with dimensionless frequency $a_0 \in [0.1, 3]$ and aspect ratio $L/B \in [1, 2]$; uniform half-space $HL/B = \infty$, (a) surface block $ZE/B=0$; (b) embedded block $ZE/B=1$

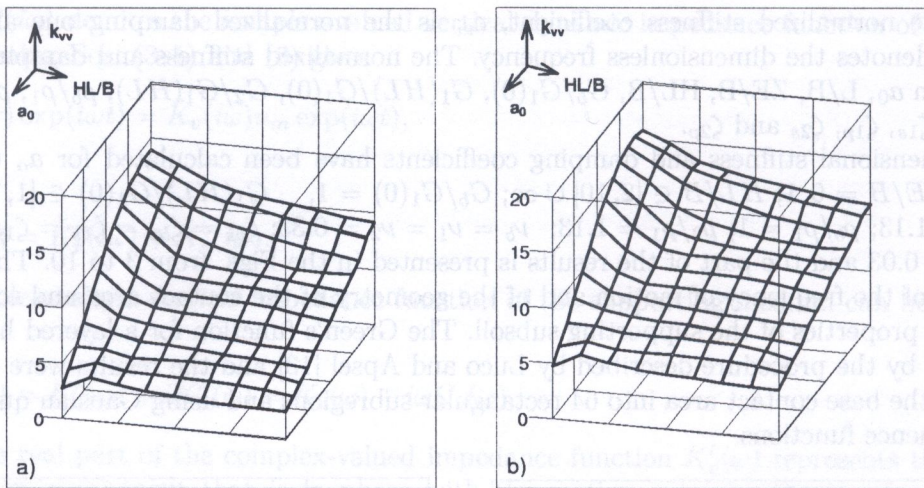


Fig. 5. Variation of normalized stiffness coefficient k_{vv} with dimensionless frequency $a_o \in [0.1, 3]$ and the ratio $HL/B \in [2, 10]$; layered half-space $G_1(HL)/G_1(0) = 4$, $L/B = 1$, (a) surface block $ZE/B = 0$; (b) embedded block $ZE/B = 1$

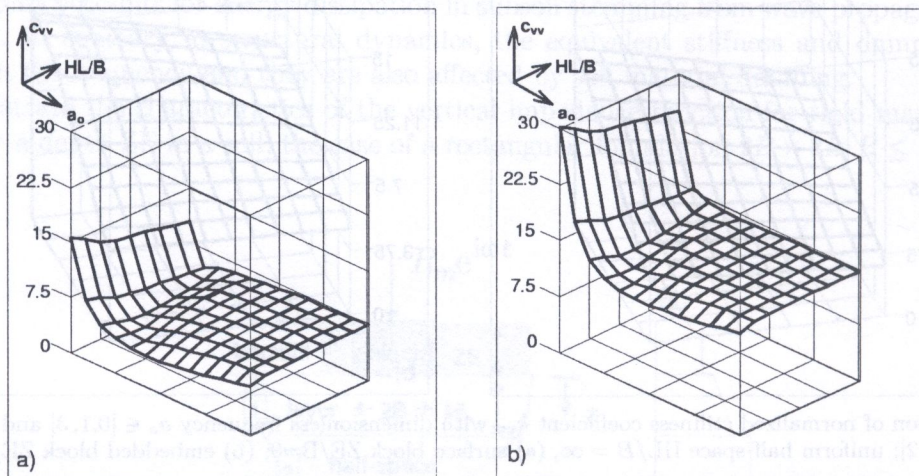


Fig. 6. Variation of normalized damping coefficient c_{vv} with dimensionless frequency $a_o \in [0.1, 3]$ and the ratio $HL/B \in [2, 10]$; layered half-space $G_1(HL)/G_1(0) = 4$, $L/B = 1$, (a) surface block $ZE/B = 0$; (b) embedded block $ZE/B = 1$

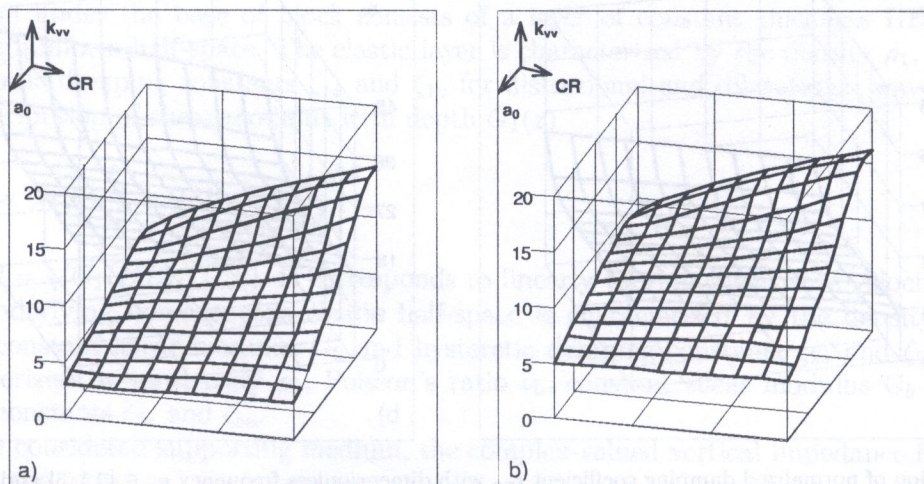


Fig. 7. Variation of normalized stiffness coefficient k_{vv} with dimensionless frequency $a_o \in [0.1, 3]$ and the contrast ratio $CR = \sqrt{G_1(HL)/G_1(0)} \in [1, 3.25]$; layered half-space $HL/B = 5$, $L/B = 1$, (a) surface block $ZE/B = 0$; (b) embedded block $ZE/B = 1$

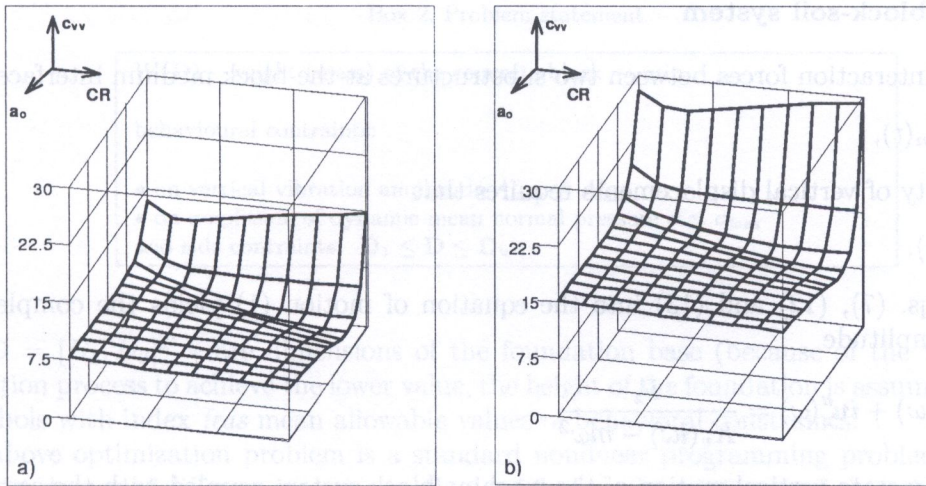


Fig. 8. Variation of normalized damping coefficient c_{vv} with dimensionless frequency $a_o \in [0.1, 3]$ and the contrast ratio $CR = \sqrt{G_1(HL)/G_1(0)} \in [1, 3.25]$; layered half-space $HL/B=5$, $L/B=1$, (a) surface block $ZE/B=0$; (b) embedded block $ZE/B=1$

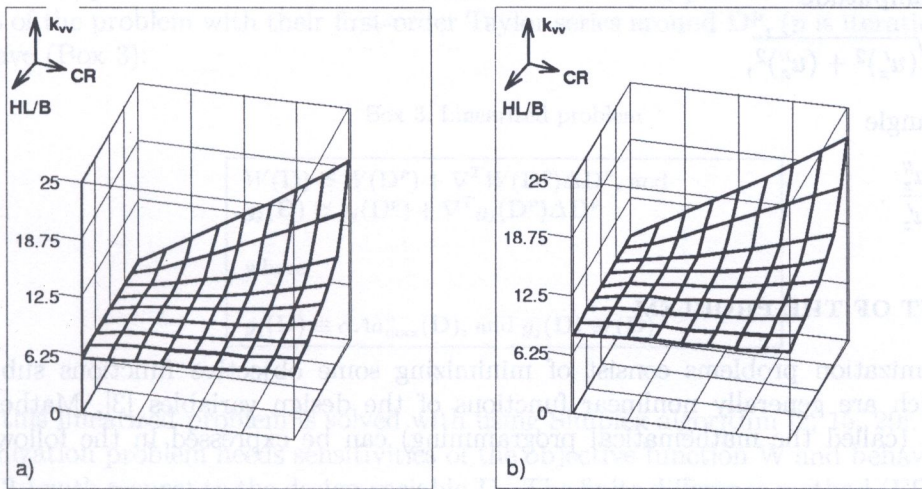


Fig. 9. Variation of normalized stiffness coefficient k_{vv} with the ratios $HL/B \in [2, 10]$ and $CR \in [1, 3]$; layered half-space $a_o = 1$, $L/B=1$, (a) surface block $ZE/B=0$; (b) embedded block $ZE/B=1$

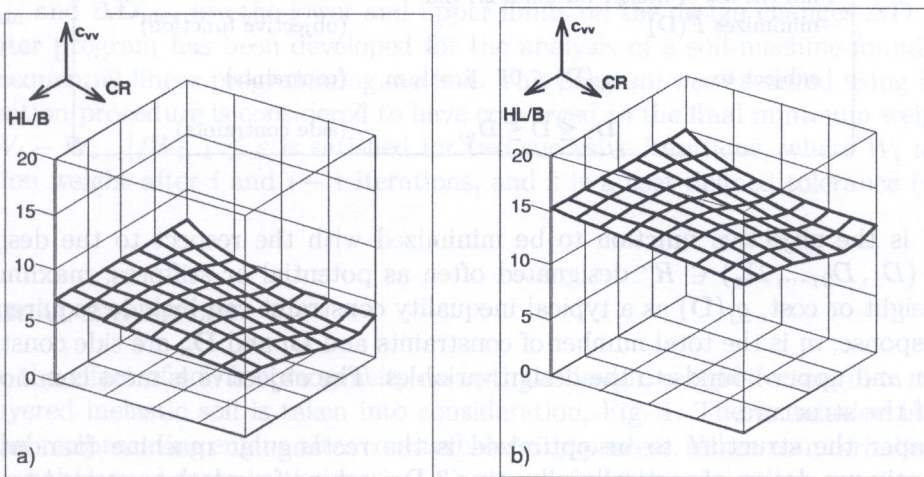


Fig. 10. Variation of normalized damping coefficient c_{vv} with the ratios $HL/B \in [2, 10]$ and $CR \in [1, 3]$; layered half-space $a_o = 1$, $HL/B=1$, (a) surface block $ZE/B=0$; (b) embedded block $ZE/B=1$

2.3. Machine-block-soil system

Equilibrium of interaction forces between two substructures at the block medium interface leads to

$$R_z(t) = -R_m(t), \tag{12}$$

and compatibility of vertical displacements requires that

$$u_z(t) = u_m(t). \tag{13}$$

Substituting Eqs. (7), (12) and (13) into the equation of motion (1) yields the complex-valued displacement amplitude

$$u_z(i\omega) = u'_z(\omega) + iu''_z(\omega) = \frac{P_z}{\tilde{K}_v(i\omega) - m\omega^2}. \tag{14}$$

Then, the steady-state vertical motion of the machine-block system coupled with the semi-infinite supporting medium is given in the form

$$u_z(t) = |u_z(i\omega)| \exp[i(\omega t + \Theta)], \tag{15}$$

where the real amplitude

$$|u_z(i\omega)| = \sqrt{(u'_z)^2 + (u''_z)^2}, \tag{16}$$

and the phase angle

$$\Theta = \arctan \frac{u''_z}{u'_z}. \tag{17}$$

3. STATEMENT OF THE PROBLEM

Structural optimization problems consist of minimizing some objective functions subjected to constraints which are generally nonlinear functions of the design variables [3]. Mathematically such problems (called the mathematical programming) can be expressed in the following form (Box 1):

Box 1. Mathematical programming

Find the set of design variables \mathbf{D} , that	
minimizes $F(\mathbf{D})$	(objective function)
subject to	$g_j(\mathbf{D}) \leq 0, \quad j = 1, m,$ (constraints)
	$\mathbf{D}_l \leq \mathbf{D} \leq \mathbf{D}_u,$ (side constraints)

where $F(\mathbf{D})$ is the objective function to be minimized with the respect to the design variables vector $\mathbf{D} = (D_1, D_2, \dots, D_n) \in R^n$ designated often as potential or stiffness, maximum stress or volume or weight or cost, $g_j(\mathbf{D})$ as a typical inequality constraint can include requirements on the structural response, m is the total number of constraints and \mathbf{D}_l and \mathbf{D}_u are side constraints which provide lower and upper bounds to the design variables. The objective is most commonly taken as the weight of the structure.

In this paper the structure to be optimized is the rectangular machine foundation and the problem of optimum design of vertically vibrating 3-D machine foundation coupled to layered half-space can be stated as follows (Box 2.):

Box 2. Problem statement

$W(\mathbf{D})$ – weight (mass) of the concrete block \rightarrow min

behavioural constraints:

- on vertical vibration amplitude $A_{\max}^v \leq A_{\text{feas}}^v$
 - on amplitude of dynamic mean normal pressure $\sigma \leq \sigma_{\text{feas}}$
- and side constraints $\mathbf{D}_1 \leq \mathbf{D} \leq \mathbf{D}_u$,

where: $\mathbf{D} = [D_1, D_2]^T$ – are dimensions of the foundation base (because of the tendency of the optimization process to achieve the lower value, the height of the foundation is assumed as constant), and symbols with index *feas* mean allowable values of behavioral constraints.

The above optimization problem is a standard nonlinear programming problem [1, 3, 18, 27]. There exist dozens of different iterative methods of finding the minimum of objective function with inequality constraints. For efficient structural systems the approximate concepts method is widely used. Linear, hyperbolic as well as hybrid formulations are used for the approximation. In this paper an iterative application of a sequential linear programming (SLP) has been applied [15, 29]. Direct linear approximations on nonlinear functions are accomplished by replacing the nonlinear functions of the problem with their first-order Taylor series around \mathbf{D}^p , (p is iteration number), [1]. So, we have (Box 3):

Box 3. Linearized problem

$$W(\mathbf{D}) \cong W(\mathbf{D}^p) + \nabla^T W(\mathbf{D}^p) \Delta \mathbf{D}^p, \text{ and}$$

$$g_j(\mathbf{D}) \cong g_j(\mathbf{D}^p) + \nabla^T g_j(\mathbf{D}^p) \Delta \mathbf{D}^p$$

where

$$g_j(\mathbf{D}) \equiv \sigma A_{\max}^v(\mathbf{D}), \text{ and } g_j(\mathbf{D}) \equiv (\mathbf{D})$$

Then this linearized problem is solved with using Simplex algorithm [2, 15, 29]. The solution to the optimization problem needs sensitivities of the objective function W and behaviour constraints (see Box 2.) with respect to the design variable D_i . The finite difference method (FDM) is adopted to obtain the gradients of the objective function W and behavioural constraints g_j . It is essential to add a set of *move limits* to the constraints of the SLP problem in order to control a stability and convergence of the algorithm [4, 12]. These *move limits* are specified as $\Delta \mathbf{D}_{\min} \leq \Delta \mathbf{D} \leq \Delta \mathbf{D}_{\max}$, where $\Delta \mathbf{D}_{\min}$ and $\Delta \mathbf{D}_{\max}$ are the lower and upper limits on the design changes $\Delta \mathbf{D}$ respectively.

A computer program has been developed for the analysis of a soil-machine-foundation system and for the sequential linear programming method. This program was executed using IBM PC/AT. The optimization procedure is considered to have converged to the final minimum weight when the condition $|W_i - W_{i-1}|/W_{i-1} \leq \varepsilon$ is satisfied for two successive iterations, where W_i and W_{i-1} are the foundation weight after i and $i - 1$ iterations, and ε is a user defined tolerance ($\varepsilon = 0.01\%$ in this paper).

4. NUMERICAL EXAMPLES

To illustrate the effect of soil inhomogeneity on optimal design, a rigid rectangular machine foundation on layered inelastic soil is taken into consideration, Fig. 1. The foundation is excited by a single cylinder reciprocating engine after counterbalancing process. When counterbalancing is done, the resulting unbalanced force in the vertical direction of piston motion has a primary as well as secondary components (see Box 4).

Box 4. Input data and limiting values of constraints

<p>(1) <i>machine data:</i> mass of machine = 1400.0 kg, total reciprocating mass $M_B = 10.8$ kg, crank length $r = 0.075$ m, length of connecting rod $l = 0.3$ m, operating speed = 1200 rpm, unbalanced vertical force: $F_z = M_B r \omega^2 \cos \omega t + M_B (r^2 \omega^2 / l) \cos 2\omega t$</p> <p>(2) <i>block data:</i> density of concrete block = 2400.0 kg/m³, height HB = 2.0 m, thickness of base slab HP = 0.5 m, constant dimensions of top part of block: YD = 2.0 m, XD = 3.0 m,</p> <p>(3) <i>backfill data:</i> thickness of backfill layer ZE = 0.0 and 1.0 m, dynamic shear modulus $G_b = 30000.0$ kN/m², density $\rho_b = 1350.0$ kg/m³, hysteretic damping constants: $\zeta_{bs} = \zeta_{bp} = 0.05$,</p>	<p>(4) <i>soil below the base of block:</i> <i>layer</i> thickness HL = 2, 3, 4, 5, 6, 7, 8, 9 and 10 m, shear modulus $G_1(0) = 40000.0$ kN/m² $G_1(\text{HL}) = CR^2 \times G_1(0)$ CR = 1.0, 1.25, 1.5, 1.75, 2.0, 2.25, 2.5, 2.75 and 3.0 Poisson's ratio $\nu_1 = 0.33$, density $\rho_1 = 1650.0$ kg/m³, hysteretic damping constants $\zeta_{1s} = \zeta_{1p} = 0.05$. <i>underlying half-space</i> shear modulus $G_2 = 1.13G_1(\text{HL})$ Poisson's ratio $\nu_2 = \nu_1$, density $\rho_2 = 1.13 \rho_1$, hysteretic damping constants $\zeta_{2s} = \zeta_{2p} = 0.03$.</p> <p>(5) <i>limiting values of constraints:</i> vertical displacement amplitude limit $A_{\text{feas}}^v = 30.0 \times 10^{-6}$ m, stresses in the soil limit $\sigma_{\text{feas}} = 150.0$ kN/m², size limits: $3.0 \text{ m} \leq D_1 \leq 5.0 \text{ m}$, $2.0 \text{ m} \leq D_2 \leq 4.0 \text{ m}$.</p>
---	---

The soil under the base of block consists of a layer of constant thickness HL bonded to an underlying uniform half-space. The inelastic layer is characterized by a shear modulus $G_1(z)$ varying with depth according to equation (10), density ρ_1 , Poisson's ratio ν_1 , and hysteretic damping constants ζ_{1s} and ζ_{1p} for distortional and dilatational waves, respectively.

The underlying homogeneous inelastic half-space is characterized by the constant shear modulus G_2 , density ρ_2 , Poisson's ratio ν_2 , and hysteretic damping constants ζ_{2s} and ζ_{2p} . The backfill is characterized by its constant shear modulus G_b , density ρ_b , Poisson's ratio ν_b , and hysteretic damping constants ζ_{bs} , ζ_{bp} . The design data parameters and limiting values of constraints are summarized in Box 4.

The calculations were performed for two values of embedment ZE, nine values of layer thickness HL, and nine values of contrast ratio $CR = \sqrt{G_1(\text{HL})/G_1(0)}$, where $G_1(0)$ and $G_1(\text{HL})$ are the shear modulus at the top and at the bottom of the layer, respectively.

Increase of the layer thickness and contrast ratio changes the stiffness and damping coefficients of the inhomogeneous soil medium compared with the uniform one. Furthermore, the backfill surrounding the foundation alters its dynamic response by increasing the stiffness and damping coefficients of the subsoil. The results of the optimization process are summarized in Tables 1 and 2 where the case $CR = 1$ corresponds to a uniform supporting medium characterized by the layer properties.

The effect of the subsoil inhomogeneity and depth of embedment on the objective function is shown in Fig. 11. For some inhomogeneous soil profiles, the minimal mass of the foundation is greater compared to the uniform one. It is important from practical point of view, because an underestimation of the mass of block will lead to failure of the machine-foundation-soil system. The worst case for surface foundation corresponds to the layer thickness HL = 3 m and the contrast ratio $CR = 2$. The minimum of the optimal objective function also exists for HL = 3 m and $CR = 3$, when the decrease of vibration amplitude due to increase of soil stiffness is greater than its increase caused by reduction of radiation damping, with reference to a uniform soil. The results for embedded foundation create a nearly flat surface. It is worth to note that embedding the foundation into the soil increase the total foundation-soil-interface and more energy is transmitted to surrounding medium and nearby structures. Limiting amplitude of soil vibrations in the vicinity

of embedded machine foundation can change results presented in Fig. 11b. It is remarkable that the stress constraints are never active during the optimization process. To optimal rectangular shape of block corresponds the appropriate stiffness and damping coefficients of the supporting medium. They are shown in Figs. 12, 13, 14 and 15, and illustrate the way that the dynamic properties of layered soil control the optimization process.

Table 1. Optimal design variables $D_1 \times D_2$ [m×m] for surface foundation

CR	HL = 3 [m]	4 [m]	5 [m]	6 [m]	7 [m]	8 [m]	9 [m]	10 [m]
1.00	3.19 × 3.00 (33072.5)	3.19 × 3.00 (33072.5)	3.19 × 3.00 (33072.5)	3.19 × 3.00 (33072.5)	3.19 × 3.00 (33072.5)	3.19 × 3.00 (33072.5)	3.19 × 3.00 (33072.5)	3.19 × 3.00 (33072.5)
1.25	3.58 × 3.20 (35353.9)	3.48 × 3.14 (34715.4)	3.41 × 3.05 (34069.7)	3.36 × 3.01 (33766.9)	3.34 × 3.01 (33673.9)	3.34 × 3.01 (33683.1)	3.36 × 3.00 (33692.1)	3.36 × 3.00 (33690.4)
1.50	3.83 × 3.43 (37365.3)	3.75 × 3.36 (36708.7)	3.59 × 3.26 (35500.6)	3.50 × 3.14 (34765.1)	3.45 × 3.09 (34388.7)	3.42 × 3.08 (34267.7)	3.42 × 3.07 (34198.1)	3.41 × 3.06 (34128.1)
1.75	4.09 × 3.58 (39178.1)	4.04 × 3.55 (38810.6)	3.81 × 3.41 (37221.0)	3.66 × 3.29 (36067.5)	3.55 × 3.21 (35268.8)	3.52 × 3.16 (34927.2)	3.50 × 3.13 (34725.4)	3.47 × 3.10 (34542.4)
2.00	4.53 × 3.50 (40625.4)	4.43 × 3.57 (40590.7)	4.05 × 3.57 (38951.6)	3.86 × 3.45 (37559.9)	3.70 × 3.33 (36357.3)	3.63 × 3.25 (35729.5)	3.57 × 3.21 (35373.1)	3.51 × 3.16 (34895.9)
2.25	5.00 × 3.11 (40277.4)	5.00 × 3.12 (40347.7)	4.39 × 3.56 (40387.4)	4.07 × 3.59 (39131.9)	3.87 × 3.46 (37685.1)	3.75 × 3.36 (36703.9)	3.68 × 3.30 (36152.0)	3.63 × 3.24 (35685.4)
2.50	5.00 × 2.24 (35017.4)	5.00 × 2.71 (37846.4)	5.00 × 3.16 (40555.0)	4.34 × 3.65 (40581.6)	4.05 × 3.62 (39212.8)	3.90 × 3.48 (37884.6)	3.79 × 3.40 (37068.6)	3.71 × 3.33 (36415.4)
2.75	4.41 × 2.00 (32191.3)	5.00 × 2.24 (35033.1)	5.00 × 2.93 (39201.1)	5.00 × 3.29 (41322.2)	4.29 × 3.73 (40815.8)	4.05 × 3.65 (39304.9)	3.92 × 3.51 (38144.4)	3.82 × 3.41 (37244.8)
3.00	3.94 × 2.00 (31053.1)	4.82 × 2.00 (33170.0)	5.00 × 2.56 (36969.4)	5.00 × 3.23 (40978.0)	5.00 × 3.44 (42212.1)	4.27 × 3.77 (40950.4)	4.08 × 3.64 (39431.5)	3.93 × 3.51 (38188.5)

(...) – optimal objective function (mass of foundation) in [kg]

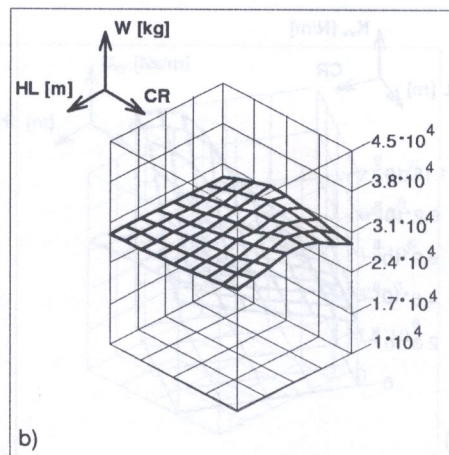
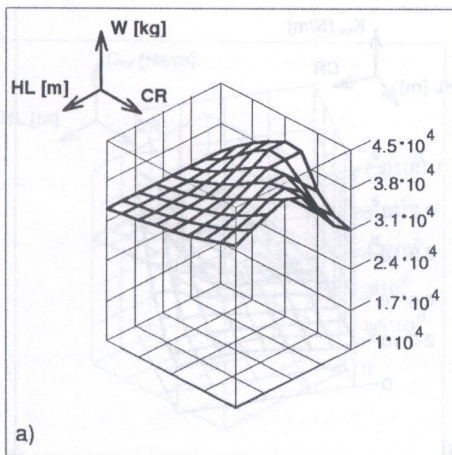


Fig. 11. Optimal objective function W [kg] versus $HL \in [3, 10]m$ and $CR \in [1, 3]$; a) surface foundation, b) embedded foundation

Table 2. Optimal design variables $D_1 \times D_2$ [m×m] for embedded foundation ($ZE = 1.0$ m)

CR	HL = 3 [m]	4 [m]	5 [m]	6 [m]	7 [m]	8 [m]	9 [m]	10 [m]
1.00	3.00 × 2.05 (28964.9)	3.00 × 2.05 (28964.9)	3.00 × 2.05 (28964.9)	3.00 × 2.05 (28964.9)	3.00 × 2.05 (28964.9)	3.00 × 2.05 (28964.9)	3.00 × 2.05 (28964.9)	3.00 × 2.05 (28964.9)
1.25	3.00 × 2.35 (30068.3)	3.00 × 2.25 (29708.7)	3.00 × 2.17 (29426.4)	3.00 × 2.14 (29311.2)	3.00 × 2.13 (29265.8)	3.00 × 2.12 (29229.8)	3.00 × 2.11 (29204.2)	3.00 × 2.11 (29189.8)
1.50	3.02 × 2.59 (31004.3)	3.00 × 2.48 (30513.7)	3.00 × 2.34 (30034.7)	3.00 × 2.26 (29740.1)	3.00 × 2.21 (29571.3)	3.00 × 2.18 (29441.2)	3.00 × 2.15 (29352.5)	3.00 × 2.14 (29307.0)
1.75	3.24 × 2.58 (31618.9)	3.09 × 2.62 (31308.6)	3.00 × 2.54 (30747.9)	3.00 × 2.40 (30253.0)	3.00 × 2.31 (29917.2)	3.00 × 2.24 (29663.4)	3.00 × 2.19 (29493.9)	3.00 × 2.17 (29406.8)
2.00	4.14 × 2.00 (31530.6)	3.33 × 2.59 (31934.1)	3.10 × 2.66 (31488.0)	3.00 × 2.57 (30835.8)	3.00 × 2.43 (30333.8)	3.00 × 2.32 (29956.9)	3.00 × 2.25 (29704.9)	3.00 × 2.21 (29568.3)
2.25	3.93 × 2.00 (31023.7)	4.31 × 2.00 (31946.4)	3.09 × 2.67 (32160.5)	3.00 × 2.56 (31487.7)	3.00 × 2.57 (30834.4)	3.00 × 2.43 (30336.9)	3.00 × 2.33 (30000.0)	3.00 × 2.28 (29805.8)
2.50	3.62 × 2.00 (30304.5)	4.18 × 2.00 (31629.2)	4.52 × 2.00 (32438.7)	3.20 × 2.76 (32175.1)	3.07 × 2.67 (31429.0)	3.00 × 2.56 (30816.8)	3.00 × 2.44 (30394.8)	3.00 × 2.37 (30132.0)
2.75	3.32 × 2.00 (29564.0)	3.96 × 2.00 (31098.8)	4.49 × 2.00 (32384.9)	3.14 × 3.00 (32914.7)	3.20 × 2.74 (32109.5)	3.09 × 2.65 (31406.5)	3.00 × 2.58 (30902.0)	3.00 × 2.49 (30563.0)
3.00	3.04 × 2.00 (28902.5)	3.71 × 2.00 (30504.3)	4.37 × 2.00 (32083.1)	4.76 × 2.00 (33024.7)	3.15 × 3.00 (32936.9)	3.19 × 2.74 (32096.6)	3.10 × 2.67 (31527.8)	3.00 × 2.49 (31114.5)

(...) – optimal objective function (mass of foundation) in [kg]

The sensitivity of an optimum to problem parameters can be estimated by general methods, e.g. [30]. But the considered optimization problem is small scale and the reoptimization has been used for specified changes of soil profile parameters.

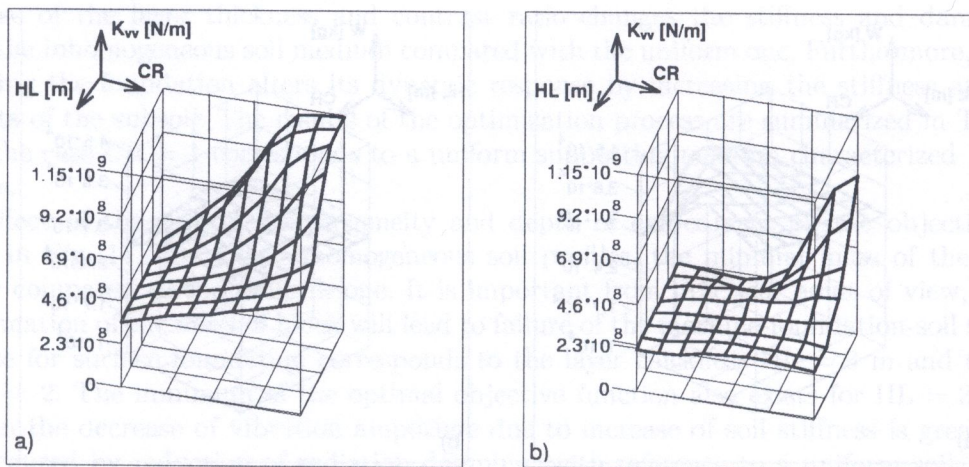


Fig. 12. Stiffness coefficient of layered medium versus $HL \in [3, 10]$ m and $CR \in [1, 3]$; surface foundation-optimal design, (a) primary component, (b) secondary component

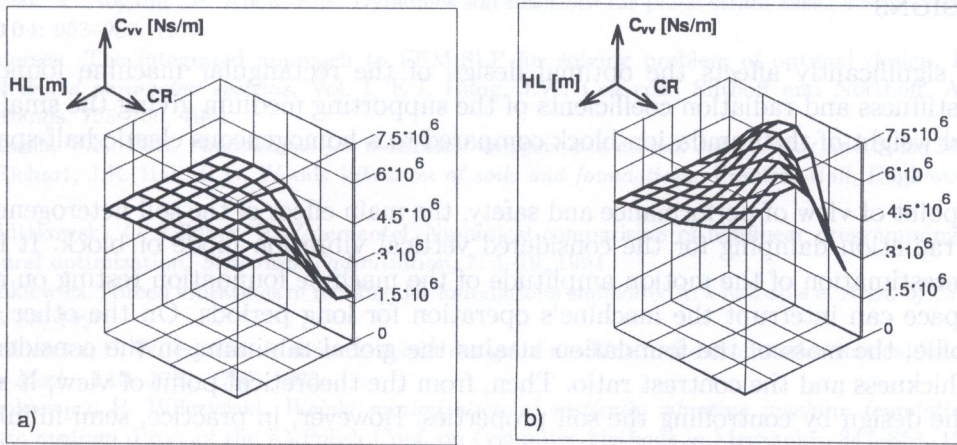


Fig. 13. Damping coefficient of layered medium versus $HL \in [3, 10]m$ and $CR \in [1, 3]$; surface foundation-optimal design, (a) primary component, (b) secondary component

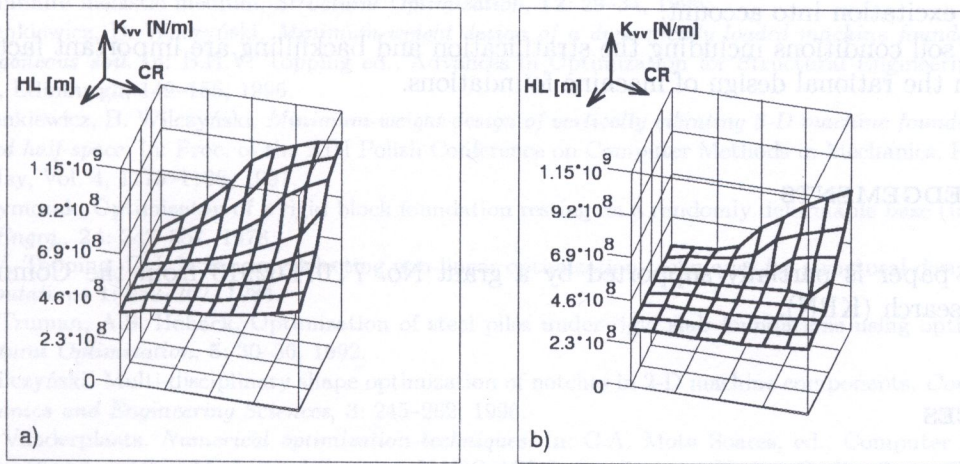


Fig. 14. Stiffness coefficient of layered medium versus $HL \in [3, 10]m$ and $CR \in [1, 3]$; surface foundation-optimal design, (a) primary component, (b) secondary component

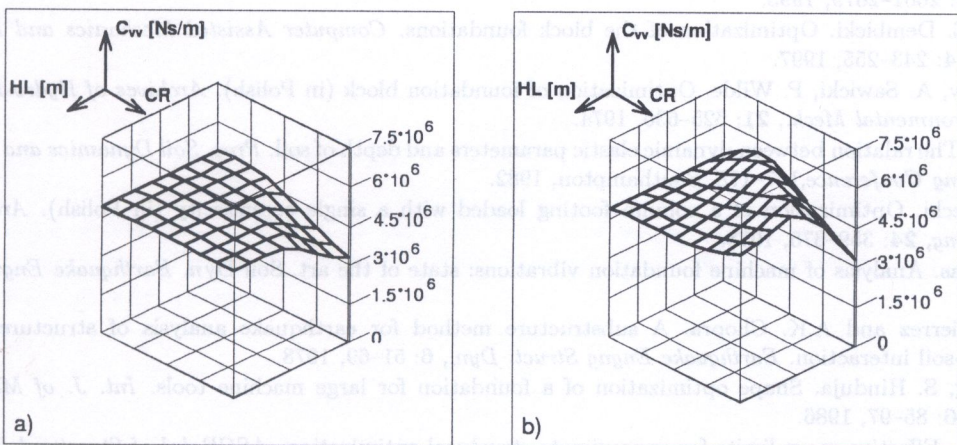


Fig. 15. Damping coefficient of layered medium versus $HL \in [3, 10]m$ and $CR \in [1, 3]$; surface foundation-optimal design, (a) primary component, (b) secondary component

5. CONCLUSIONS

Soil layering significantly affects the optimal design of the rectangular machine foundation. It modifies the stiffness and radiation coefficients of the supporting medium giving the smaller or the larger optimal weight of the foundation block compared to a homogeneous elastic half-space model of soil.

From the point of view of performance and safety, the main effect of the soil heterogeneity is the reduction of radiation damping for the considered vertical vibration mode of block. It is evident that the underestimation of the motion amplitude of the machine foundation resting on a uniform elastic half-space can interrupt the machine's operation for long periods. On the other hand, for some soil profile, the mass of the foundation attains the global minimum in the considered range of the layer thickness and the contrast ratio. Then, from the theoretical point of view, it is possible to improve the design by controlling the soil properties. However, in practice, semi-infinite nature of the soil medium and uncertainties existing in the estimation of dynamic soil parameters should be taken into account.

The method of dynamic analysis of the machine-block-soil system must adequately take the shape of the block-soil interface, the amount of embedment, the nature of the soil profile and the frequency of excitation into account.

The local soil conditions including the stratification and backfilling are important factors to be considered in the rational design of machine foundations.

ACKNOWLEDGEMENTS

The present paper is partially supported by a grant No. 7T07E02913 from the Committee for Scientific Research (KBN).

REFERENCES

- [1] J-F.M. Barthelemy, R.T. Haftka. Approximation concepts for optimum structural design-a review, *Structural Optimization*, 5: 129-144, 1993.
- [2] J. Best, K. Ritter. *Linear Programming*. Prentice-Hall Englewood Cliffs, New York, 1985.
- [3] A.M. Brandt et al. *Foundations of Optimum Design in Civil Engineering*. PWN, Warszawa, Martinus Nijhoff Publishers, Dordrecht, 1989.
- [4] T.-Y. Chen. Calculation of the move limits for the sequential linear programming method. *Int. Jnl Num. Meth. Engrg*, 36: 2661-2679, 1993.
- [5] T. Chi, E. Dembicki. Optimization of the block foundations. *Computer Assisted Mechanics and Engineering Sciences*, 4: 243-255, 1997.
- [6] E. Filipow, A. Sawicki, P. Wilde. Optimization of foundation block (in Polish). *Archives of Hydro-Engineering and Environmental Mech.*, 21: 625-636, 1974.
- [7] P. Fulan. The relation between dynamic elastic parameters and depth of soil. *Proc. Soil Dynamics and Earthquake Engineering Conference*, 167-178, Southampton, 1982.
- [8] A. Garstecki. Optimization of a column footing loaded with a single eccentricity (in Polish). *Arch. of Civil Engineering*, 24: 359-375, 1978.
- [9] G. Gazetas. Analysis of machine foundation vibrations: state of the art. *Soil Dyn. Earthquake Engng*, 2: 2-42, 1983.
- [10] J.A. Gutierrez and A.K. Chopra. A substructure method for earthquake analysis of structures including structure-soil interaction. *Earthquake Engng Struct. Dyn.*, 6: 51-69, 1978.
- [11] Z. Huang, S. Hinduja. Shape optimization of a foundation for large machine tools. *Int. J. of Machine Tool Design*, 26: 85-97, 1986.
- [12] U. Kirsch. Effective move limits for approximate structural optimization. *ASCE Jnl of Structural Engineering*, 123: 210-217, 1997.
- [13] J.E. Luco, R.J. Apsel. On the Green's functions for layered half-space: part I. *Bull. Seism. Soc. Am.*, 73: 909-924, 1983.

- [14] M. Novak, T. Nogami, F. Aboul-Ella. Dynamics soil reactions for plane strain case. *ASCE Jnl of Engng Mech. Div.*, **104**: 953–959, 1978.
- [15] P. Pedersen. The integrated approach to FEM-SLP for solving problem of optimal design. In: *Optimization of distributed parameter systems*, Vol. I, E.J. Haug, J.W. Cea eds., Sijthoff and Northhoff, Amsterdam, the Netherlands, 735–756, 1981.
- [16] S. Prakash, V.K. Puri. *Foundations for machines: analysis and design*. John Wiley and Sons, New York, 1988.
- [17] F.E. Richart, J.R. Hall, R.D. Woods. *Vibration of soils and foundations*. Prentice-Hall, Englewood Cliffs, N.Y., 1970.
- [18] K. Schittkowski, C. Zillober, R. Zotemantel, Numerical comparison of nonlinear programming algorithms for structural optimization, *Structural Optimization*, **7**: 1–19, 1994.
- [19] Z. Sienkiewicz. Forced vibrations of rectangular foundations embedded in a half-space. *Arch. of Civil Engineering*, **38**: 35–58, 1996.
- [20] Z. Sienkiewicz, B. Wilczyński. Minimum-weight design of machine foundation under vertical load, *ASCE Jnl. of Engng Mech.*, **119**: 1781–1797, 1993.
- [21] Z. Sienkiewicz, B. Wilczyński. *Weight minimization of vertically vibrating machine foundation embedded in inelastic medium*. Proc. of the XI Polish Conf. on Computer Methods in Mechanics, 847–854, 1993.
- [22] Z. Sienkiewicz, B. Wilczyński. *Shape optimization of dynamically loaded machine foundation coupled to semi-infinite inelastic medium*. In: N. Olhoff and G.I.N. Rozvany, eds., Proc. First World Congress of Structural and Multidisciplinary Optimization, Goslar, May 28–June 2, 1995, Germany, 653–658, 1995.
- [23] Z. Sienkiewicz, B. Wilczyński. Shape optimization of a dynamically loaded machine foundation coupled to a semi-infinite inelastic medium, *Structural Optimization*, **12**: 29–34, 1996.
- [24] Z. Sienkiewicz, B. Wilczyński. *Minimum-weight design of a dynamically loaded machine foundation on an inhomogeneous soil*. In: B.H.V. Topping ed., *Advances in Optimization for Structural Engineering*, Civil-Comp Press, Edinburgh, 149–155, 1996.
- [25] Z. Sienkiewicz, B. Wilczyński, *Minimum-weight design of vertically vibrating 3-D machine foundation coupled to layered half-space*. In: Proc. of the XIII Polish Conference on Computer Methods in Mechanics, Poznań, Poland, 5–8 May, Vol. 4, 1179–1186, 1997.
- [26] C. Szymczak. Optimizaton of a rigid block foundation resting on a randomly deformable base (in Polish). *Arch. Civ. Engrg.*, **24**: 347–357, 1978.
- [27] B.H.V. Topping, D.J. Robinson. Selecting non-linear optimization techniques for structural design. *Engineering Computations* **1**: 252–262, 1984.
- [28] K.Z. Truman, A.S. Hoback. Optimization of steel piles under rigid slab foundations using optimality criteria. *Structural Optimization*, **5**: 30–36, 1992.
- [29] B. Wilczyński. Multi-disciplinary shape optimization of notches in 2-D machine components. *Computer Assisted Mechanics and Engineering Sciences*, **3**: 245–262, 1996.
- [30] G.N. Vanderplaats. *Numerical optimization techniques*. In: C.A. Mota Soares, ed., *Computer Aided Optimal Design: Structural and Mechanical Systems*. NATO ASI Series, Springer-Verlag, Berlin, Series F., Vol. 27, 197–239, 1987.
- ions, e.g. in lubrication of porous bearings, ground water hydrology and in industrial filtration processes where a porous matrix is used inside the fluid passage. Several geophysical and energy engineering applications were elaborated by Kim *et al.* [8]. Secondly, nutritional problems in the alimentary canal such as indigestion, constipation, diarrhoea, etc., could be effectively rectified if the biomechanics of chyme absorption in the small intestine (which can be easily simulated using this model) is well understood.
- Berman [1] presented an exact solution of the Navier-Stokes equations that describe the steady flow in a channel driven by suction at the walls. He employed the Hiemenz [7] similarity form of solution in order to reduce the problem to a fourth order nonlinear ordinary differential equation. In this regard numerous authors e.g. Terrill and Thomas [12], Durbin and Brady [4], Zagarola and Banks [14], Makinde [9], etc., have developed and generalised this exact solution for the case flow in a pipe driven by uniform wall suction. The most amazing and significant result in their study is the presence of a region bounded by two turning points in the solution field where no real solution of the given type exist.
- However, in the present work, the suction driven flow in a pipe filled with porous media is considered. In this type of study, the common approach has been to use Darcy's law in the porous medium (generally with low permeabilities) together with the Navier-Stokes equations.
- Our objective is to study the effect of porous media on the bifurcation that takes place in the flow field as the suction Reynolds number increases. To achieve this goal, we have employed a novel computational approach to the study of bifurcations presented by Drazin and Bourgin [5]. The technique relies on the use of power series in the bifurcation parameter for a particular